

Self-Powered Acoustic Source Locator in Underwater Environment Based on Organic Film Triboelectric Nanogenerator

Aifang Yu^{1†}, Ming Song^{1†}, Yan Zhang¹, Yang Zhang¹, Libo Chen¹, Junyi Zhai¹ (✉) and Zhong Lin Wang^{1,2} (✉)

Nano Res., **Just Accepted Manuscript** • DOI: 10.1007/s12274-014-0559-z
<http://www.thenanoresearch.com> on August 9, 2014

© Tsinghua University Press 2014

Just Accepted

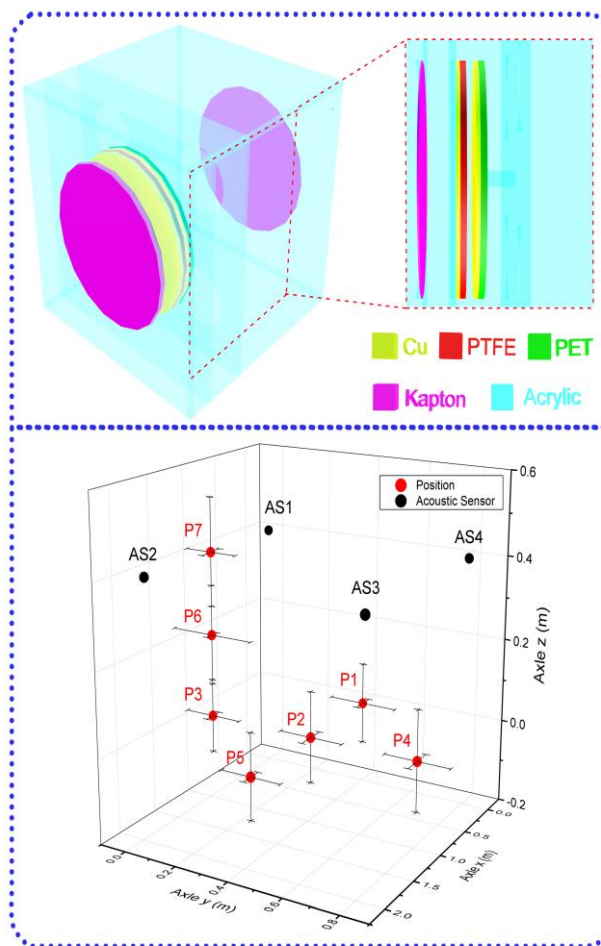
This is a “Just Accepted” manuscript, which has been examined by the peer-review process and has been accepted for publication. A “Just Accepted” manuscript is published online shortly after its acceptance, which is prior to technical editing and formatting and author proofing. Tsinghua University Press (TUP) provides “Just Accepted” as an optional and free service which allows authors to make their results available to the research community as soon as possible after acceptance. After a manuscript has been technically edited and formatted, it will be removed from the “Just Accepted” Web site and published as an ASAP article. Please note that technical editing may introduce minor changes to the manuscript text and/or graphics which may affect the content, and all legal disclaimers that apply to the journal pertain. In no event shall TUP be held responsible for errors or consequences arising from the use of any information contained in these “Just Accepted” manuscripts. To cite this manuscript please use its Digital Object Identifier (DOI®), which is identical for all formats of publication.

Self-Powered Acoustic Source Locator in Underwater Environment Based on Organic Film Triboelectric Nanogenerator

Aifang Yu^{1, †}, Ming Song^{1, †}, Yan Zhang¹, Yang Zhang¹, Libo Chen¹, Junyi Zhai^{*.1} and Zhong Lin Wang^{*.1,2}

¹Beijing Institute of Nanoenergy and Nanosystems, Chinese Academy of Sciences, Beijing, 100083, China.

²School of Material Science and Engineering, Georgia Institute of Technology, Atlanta, Georgia 30332, USA.



In this paper, organic-film based triboelectric nanogenerator (TENG) was first successfully demonstrated as a self-powered and high sensitivity acoustic sensor to detect underwater target at low frequency around 100 Hz. The three dimensional coordinate of acoustic source was identified by four TENGs, self-powered active sensors, and the location of the acoustic source was determined with an error about 0.2 m.

Zhong Lin Wang, <http://www.nanoscience.gatech.edu/>

Self-Powered Acoustic Source Locator in Underwater Environment Based on Organic Film Triboelectric Nanogenerator

Aifang Yu^{1†}, Ming Song^{1†}, Yan Zhang¹, Yang Zhang¹, Libo Chen¹, Junyi Zhai¹ (✉) and Zhong Lin Wang^{1,2} (✉)

¹Beijing Institute of Nanoenergy and Nanosystems, Chinese Academy of Sciences, Beijing, 100083, China.

²School of Material Science and Engineering, Georgia Institute of Technology, Atlanta, Georgia 30332, USA.

† Authors with equal contribution and authorship order determined by coin toss.

Received: day month year

Revised: day month year

Accepted: day month year
(automatically inserted by
the publisher)

© Tsinghua University Press
and Springer-Verlag Berlin
Heidelberg 2014

KEYWORDS

triboelectric
nanogenerator,
self-powered acoustic
source locator,
underwater, three
dimensional coordinate

ABSTRACT

Detecting/sensing targets underwater has very important application in environmental study, civil engineering and national security. In this paper, organic-film based triboelectric nanogenerator (TENG) was first successfully demonstrated as a self-powered and high sensitivity acoustic sensor to detect underwater target at low frequency around 100 Hz. This innovative, cost-effective, simple-designed TENG consists of thin-film-based Cu electrode and a polytetrafluoroethylene (PTFE) film with nanostructures on surfaces. On the basis of the coupling effect between triboelectrification and electrostatic induction, the sensor generates electric output signals in response to incident sound wave. Operating at a resonance frequency of 110 Hz, under acoustic pressure of 144.2dB_{SPL}, the maximum open-circuit voltage and **short-circuit current** of the generator can respectively reach 65 V and 32 μ A underwater. The directional dependence pattern is in a bi-directional shape with total response angle of 60°. Its sensitivity is higher than -185 dB in a frequency range from 30Hz to 200Hz. The highest sensitivity is -146dB at resonance frequency. The three dimensional coordinate of acoustic source was identified by four TENGs, self-powered active sensors, and the location of the acoustic source was determined with an error about 0.2 m. This study not only expands the application fields of TENGs from atmosphere to water, but also exhibits the TENG as a promising acoustic source locator in underwater environment.

Address correspondence to Zhong Lin Wang, zlwang@gatech.edu; Junyi Zhai, jyzhai@binn.cas.cn

1 Introduction

Self-powered sensors that can function without external power have attracted increasing attention in recent years [1, 2]. They have been demonstrated as new approaches for pH [3], temperature [4], biosensor [5], toxic pollutants [6] and vibration sensing [7]. By deriving energy directly from the environment, these self-powered devices are advantageous in minimizing the size and avoiding maintenance in battery [8, 9]. Recently, an innovative triboelectric nanogenerator (TENG) [10], based on a coupling of the universally known contact electrification effect and electrostatic induction, has been extensively utilized to successfully build up cost-effective and robust self-powered sensing systems with superior performance due to the excellent high output, such as vibration sensor [11], chemical sensor [12], pressure sensor [13], tactile sensor [14], acoustic sensor [15] and et.al [16]. In these self-powered sensors, TENG automatically generates output voltage / current signals through the triboelectrification (in inner circuit) and electrostatic induction processes (in outer circuit) once it is triggered or agitated by vibration, pressure, touch and et.al. The output signal signifies the mechanical triggering or agitation and its time-dependent behavior. This is the basic principle of the TENG applied as a self-powered sensor. So far, the self-powered sensors based TENGs are in the atmospheric environment, it is important to demonstrate their applications in other environment, especially underwater.

Due to military surveillance requirements in underwater and the urgent needs to expand and utilize marine resources, underwater sound detecting/sensing technology is experiencing an unprecedented development. In order to meet these urgent needs, underwater sound transducer with high sensitivity, at low-frequency, high power and large-aperture is important [17]. Some new type sensors with unique merit were developed, including

vector acoustic sensor, sensor based on flexible organic PVDF piezoelectric film and optical fiber transducer [18, 19].

In this paper, an organic thin film TENG, which is constructed by organic film with nanostructures on surface and is based on a coupling of the universally known contact electrification effect and electrostatic induction, was successfully demonstrated as a self-powered and high sensitivity acoustic sensor to detect underwater target. The TENG automatically generates output voltage / current signals in response to incident sound wave. Under careful design of the straining conditions between the contact face of a polytetrafluoroethylene (PTFE) thin film and polytetrafluoroethylene (PET) film with sputtered copper electrode, the maximum open circuit voltage and current of the generator, operating at resonance frequency of 110 Hz and under acoustic pressure of 144 dB_{SPL}, can respectively reach 65 V and 32 μ A underwater. The highest sensitivity demonstrated is -146dB at resonance frequency. The three dimensional coordinate of an acoustic source was determined by four TENG self-powered active sensors at an error about 0.2 m. This study not only expands the application fields of TENGs from air to water, but also presents a promising candidate of high sensitivity self-powered acoustic sensor underwater which is also adaptable and cost-effective.

2 Experimental

The structure of the acoustic sensor is a sealed cubic resonance cavity. The dimension of cubic cavity is 90 mm by 90 mm by 90 mm and constructed using acrylic sheet (thickness of 5 mm). Two circular holes with diameter of 85mm locating in the front plate and back plate were covered with organic Kapton (PI) membranes, respectively. The PI film is used as sound-transparent and waterproof layer. The core of TENG is constructed by two contact faces in a circular shape with a diameter of 75mm and

embedded near the front plate of the cavity, which can be clearly seen from a lateral view as sketched in Fig. 1(a). One contact face is PTFE film with a deposited copper thin film as the back electrode, which is adhered onto an acrylic glass with circle hole. A piece of PET film with a deposited copper thin film as another contact face was adhered onto a circle acrylic glass. Figure 1(b) displays a corresponding photograph of the sensor. Surface modification on the PTFE was adopted to create vertically aligned polymer nanowires by the inductively coupled plasma (ICP) reactive ion etching. The uniformly distributed nanowire features as shown in Fig.1(c) can further increase the surface roughness and the effective surface area of the TENG for effective triboelectrification. The effective area of the TENG is about 44 cm². The output voltage of the device was measured using a Lecroy 610Zi Oscilloscope with four channels and load resistance of 10 M Ω . The output current of the device was measured using a low noise current preamplifier (Stanford Research SR570). A loud underwater speaker that provides sinusoidal sound waves was used as an acoustic source with tunable frequency and amplitude. The measurement was done in a pool with dimensions of 2 m \times 1m \times 0.5 m. The acoustic pressure level was measured by a referred acoustic sensor (reson4013).

3 Results and discussion

Figure 2 illustrates the electricity generation mechanism of the TENG. It can be explained by the combination of the triboelectrification effect and electrostatic induction. When an external sound wave is incident on the PI film, the air within the cavity is alternately compressed and expanded in response to the magnitude and frequency of the sound wave, and thus, the PTFE thin film will oscillate with air while the PET film stays still as shown in Fig. 2a. Because of the large difference in the ability to attract electrons, when the Cu contact face is in contact with the PTFE

film, surface charge transfer takes place in its original state (Fig. 2(b)). Because PTFE has a much more triboelectric negative polarity than that of the Cu contact face, electrons are injected from Cu contact face into PTFE, generating positive triboelectric charges on the Cu contact face side and negative charges on the PTFE side. Due to the wave character of sound propagation, a resulting acoustic pressure separates the PTFE thin film away from the Cu contact face. As a result, the positive triboelectric charges and the negative ones no longer coincide on the same plane and an inner dipole moment between the two contact surfaces is consequently generated, which drives free electrons to flow from the Cu electrode to the Cu contact face to screen the local electric field, producing positively induced charges on the Cu electrode (Fig. 2(c)). The flow of electrons lasts until the PTFE thin film reaches the highest point, where the corresponding separation is maximized (Fig.2 (d)). Subsequently, due to the acoustic pressure difference change, the PTFE film is pushed back toward the Cu contact face. In response to the reduced separation and thus the weakened potential drop, the free electrons in Cu contact face flow back to the Cu electrode (Fig. 2(e)). Finally, when these two plates contact each other again, there is no current flow in the external circuit, and the triboelectric charge distribution is restored to the original status (Fig. 2(b)). This is a complete cycle of electricity generation. As the PTFE thin film is bounced away from the Cu thin film again after obtaining a momentum from the sound waves, starting another cycle of electricity generation. Referring the model of two flat panel capacitors [20], the output voltage is proportional to the distance between PTFE and PET and the output current is to proportional the distance change rate of the two films.

For such a resonance cavity structure, the frequency response is of great interest for the output performance of TENG. The frequency response of the TENG's output performance underwater is shown in

Figs. 3(a) and 3(b). It can be seen that the TENG works well at low frequency range, especially around resonance frequency 110 Hz. Note the depth of water where the sensor was placed was 0.4m. Both the voltage and current present a rapid increase with an increase of frequency from 0 to 110 Hz. Then, both of them gradually dropped to their minima as the frequency increases from 110 to 200 Hz. It is noted that the drop of current versus frequency is slower than that of voltage versus frequency from 110 to 200 Hz, which is related to the fast distance change rate in high frequency. Under resonance frequency and a fixed acoustic pressure of 144 dB_{SPL}, through tuning the distance between two films, maximum output underwater was obtained. Such a distance depends on the depth at which the TENG is placed in water. Figures 3c and 3d give the **open-circuit voltage** and short-circuit current. The sensor exhibits superior electrical performance. The open-circuit voltage (V_{oc}) reaches 65 V and the short-circuit current (I_{sc}) is around 32 μ A. The open-circuit voltage is much higher than commercial PVDF acoustic sensor under the same condition, which is of benefit to detecting weak acoustic signal underwater. A further step is made toward investigating the relationship between electrical outputs and applied acoustic pressure of the optimized device. The acoustic pressure ranging from 150 dB_{SPL} to 130 dB_{SPL} is controlled and measured by the referred acoustic sensor. The electric output is highly related to the input acoustic pressures and detailed relationships are demonstrated in Fig.3 (e). As revealed, at the resonant frequency of 110 Hz, with decreasing acoustic pressure from 154.5 dB_{SPL} to 133.4 dB_{SPL}, the V_{oc} is decreased from 91 V to 7.5 V. Moreover, the V_{oc} is in a linear relationship with acoustic pressure. Therefore, the TENG also can be used as a sound pressure meter. Furthermore, because the acoustic waves decay in the course of propagation, a distance depended electric output is measured at a fixed acoustic pressure of 144 dB_{SPL} and resonant frequency of 110 Hz. It can be clearly seen that the

distance of the measured device to the acoustic source shows a tremendous impact on the electric output for acoustic energy transduction as shown in Fig. 3(f). The open-circuit voltage is decreased from 65.50 V to 0.81 V when the distance is increased from 5 cm to 100 cm. These voltage/current signals in Fig. 3 suggest the as-fabricated TENG has good response to the characteristics of acoustic source, such as frequency, acoustic pressure and distance. The TENG showed good performance as an underwater acoustic sensor.

As an acoustic sensor, the acoustical performance of the TENG was comprehensively studied. The directional dependence (directivity) pattern of the as fabricated devices was first evaluated. We anchored the device onto a rotary stage and then gradually increased the rotating angle from 0 to 360° and measured the V_{oc} at the resonant acoustic frequency of 110 Hz. The corresponding directional pattern is obtained by normalizing relative to the peak response of voltage, as illustrated in Fig. 4(a). The test results show that the pattern is in a bi-directional shape and smooth as a function of rotating angle, and the -3 dB points are at +30° and -30° off axis, producing a total response angle of 60°. This pattern can improve the measurement gain. At an incident angle of 90°, the sound pressure level is reduced to -17 dB from the maximum value on-axis. The device is most sensitive to sound incident from either 0° or 180° and least sensitive to sounds incident from angles of either 90° or 270°. The acoustical response has a dependence on the incident angle of the sound waves and rejects the contribution from other angles, which renders it a great potential in the application of directional acoustic sensors. **The asymmetrical bi-directional shape is related to the asymmetrical structure of the acoustic sensor.** One as-fabricated device not only can detect objects on the surface of water, but also objects located underwater. Sensitivity is another important parameter of acoustic sensor. The sensitivity is defined as

$$S_T = 20 \log \frac{V_{OC}^T}{V_{OC}^R} + S_R \quad (1)$$

Where S_T is the sensitivity of TENG and S_R is the sensitivity of the referred acoustic sensor. V_{OC}^T and V_{OC}^R are the open circuit voltage of the TENG and referred acoustic sensor under same acoustic environment, respectively. A commercial acoustic sensor (reson4013) with sensitivity of -216.5 dB at 110 Hz was used as referred sensor. The obtained sensitivity of TENG is higher than the level of -185 dB in the frequency range from 30 Hz to 200 Hz as shown in Fig. 4(a), which indicates that the sensor can be used at low frequency with high sensitivity. The highest sensitivity reaches -146dB at resonance frequency of 110 Hz, which is much higher than that of referred sensor. The high sensitivity of TENG to acoustic signal results from the unique electricity generation mechanism introduced above and ensures it detecting weak signal without using electrical amplifier.

Finally, TENG is demonstrated as a self-powered acoustic sensor to detect the location of acoustic source underwater in Fig. 5. These sensors do not need an external power source to drive it. Four TENGs arranged in a rectangle shape were used to construct a multichannel active sensor system in passive mode, which has the capability of locating underwater acoustic source in a three dimensional coordinate. Seven different positions in the pool were checked, as indicated in Fig. 5(a). The position coordinates of these acoustic sources (Ps) and active sensors (ASs) are given in Table S1. The sensors automatically generate an output voltage signal once they are triggered by sound wave. No preamplifier is used during the measurement process. Figure 5(b) elucidates a representative signal pattern acquired by the TENGs when acoustic source locates at position 2. We can see that when the sound wave propagates to

the TENGs, electric signals are generated and then are gradually damped. The enlarged view of signals in the insert figure reveals that sound wave arrives at AS₁ and AS₄, AS₂ and AS₃ at the same time, which is in good agreement with the real experiment case. When acoustic source is settled with various distances to the ASs, the four acoustic signals show obvious discrepancies in response starting time, as demonstrated in Figure S1. The acoustic localization algorithm presented in this work is based on the estimation of the time difference of arrival (TDOA) at pairs of acoustic sensors. The time difference between the two acquired signals is estimated by the time lag at the highest peaks of their cross-correlation functions. The cross-correlation function

$R_{Z_i, Z_j}(\tau)$ between AS_{*i*} and AS_{*j*} is defined as

$$R_{Z_i, Z_j}(\tau) = \sum_{n=1}^N Z_i(n) Z_j(n+\tau) \quad (2)$$

Where *n* is the number of the sample points. Three correlation functions of the four acquired acoustic signals in Fig. 5(b) derived from Eq. (2) were shown in Fig. 5(c). The values τ_{12} , τ_{13} and τ_{14} are obtained, and equal to -25 μ s, 34 μ s and 0 μ s, respectively. The fluctuation of τ_{12} and τ_{13} is caused by systematic error. Given the distances between the four acoustic sensors and also the in-pair time delay information, the acoustic source can be localized/positioned as the intersection of the three hyperboloids as defined by the time-distance relationship as governed by the speed of sound in water, as shown in Fig. 5(d) [21]. The corresponding experimental results are shown in Fig.5 (e). The statistical error is about 0.2 m after multiple measurements. The error mainly associates with the size of water areas, reverberation, the distance between ASs and the signal-to-noise ratio of the acquired signals. For larger water areas, like a lake, as the time difference of arrival will be more distinct, the spatial location resolution is expected to be much better than this.

4 Conclusions

In conclusion, we have developed a new type of acoustic sensor to locate underwater targets, which works based on triboelectrification effect, a universal phenomenon upon contact between two materials with opposite triboelectric polarities. Rationally designed structure, coupled with nanomaterial modification, the as-fabricated nanogenerator enables superior acoustical performance. The directional dependence pattern is in a bi-directional shape with total response angle of 60°. Its sensitivity is higher than -185 dB in a frequency range from 30 Hz to 200 Hz. The highest sensitivity is -146 dB at resonance frequency. Four generators were used to locate the three dimension coordinates of acoustic source with an error about 0.2 m. This study not only expands the application fields of TENGs from air to water, but also presents a promising candidate of high sensitivity self-powered acoustic sensor underwater which is also adaptable and cost-effective.

Acknowledgements

Research was supported by the "thousands talents" program for pioneer researcher and his innovation team, China, Beijing City Committee of science and technology(Z131100006013004) . Thanks to Dr. Jin Yang, Weiming Du, Limin Zhang, Caihong Liu, Rui Wang and Peng Li for technical support.

Electronic Supplementary Material:

Supplementary material is available in the online version of this article

References

- [1] Wang, Z. L.; Song, J. Piezoelectric nanogenerators based on zinc oxide nanowire arrays. *Science* 2006, 312, 242-246.
- [2] Wang, Z. L. Self-powered nanosensors and nanosystems. *Adv. Mater.* 2012, 24, 280-285.
- [3] Xu, S.;Qin, Y.;Xu, C.;Wei, Y.;Yang, R.; Wang, Z. L. Self-powered nanowire devices. *Nat. Nanotechnol.* 2010, 5, 366-373.
- [4] Yang, Y.; Lin, Z. H.;Hou, T.;Zhang, F.; Wang, Z. L. Nanowire-composite based flexible thermoelectric nanogenerators and self-powered temperature sensors. *Nano Res.* 2012, 5, 888-895.
- [5] Katz, E.;Buckmann, A. F.; Willner, I. Self-powered enzyme-based biosensors. *J. Am. Chem. Soc.* 2001, 123, 10752-10753.
- [6] Wen, D.;Deng, L.;Guo, S.; Dong, S. Self-powered sensor for trace Hg²⁺ detection. *Anal. Chem.* 2011, 83, 3968-3972.
- [7] Yu, A.; Jiang, P.; Lin Wang, Z. Nanogenerator as self-powered vibration sensor. *Nano Energ.* 2012, 1, 418-423.
- [8] Wang, Z. L. Self-powered nanotech. *Sci. Am.* 2008, 298, 82-87.
- [9] Akyildiz, I. F.; Jornet, J. M. Electromagnetic wireless nanosensor networks. *Nano Commun. Networks* 2010, 1, 3-19.
- [10] Fan, F. R.;Tian, Z. Q.; Wang, Z. L. Flexible triboelectric generator. *Nano Energ.* 2012, 1, 328-334.
- [11] Fan, F. R.; Lin, L.;Zhu, G.;Wu, W.;Zhang, R.; Wang, Z. L. Transparent triboelectric nanogenerators and self-powered pressure sensors based on micropatterned plastic films. *Nano Lett.* 2012, 12, 3109-3114.
- [12] Lin, L.;Xie, Y. N.;Wang, S. H.;Wu, W. Z.;Niu, S. M.;Wen, X. N.; Wang, Z. L. Triboelectric Active Sensor Array for Self-Powered Static and Dynamic Pressure Detection and Tactile Imaging. *ACS Nano* 2013, 7, 8266-8274.
- [13] Chen, J.;Zhu, G.;Yang, W. Q.;Jing, Q. S.;Bai, P.;Yang, Y.; Hou, T. C.; Wang, Z. L. Harmonic-Resonator-Based Triboelectric Nanogenerator as a Sustainable Power Source and a Self-Powered Active Vibration Sensor. *Adv. Mater.* 2013, 25, 6094-6099.
- [14] Lin, Z. H.;Zhu, G.;Zhou, Y. S.;Yang, Y.;Bai, P.;Chen, J.; Wang, Z. L. A Self-Powered Triboelectric Nanosensor for Mercury Ion Detection. *Angew.*

- Chem. Int. Ed. 2013, 52, 5065-5069.
- [15] Yang, J.;Chen, J.;Liu, Y.;Yang, W. Q.;Su, Y. J.; Wang, Z. L. Triboelectrification-Based Organic Film Nanogenerator for Acoustic Energy Harvesting and Self-Powered Active Acoustic Sensing. *Acs Nano* 2014, 8, 2649-2657.
- [16] Zhang, H.;Yang, Y.;Su, Y.;Chen, J.;Adams, K.;Lee, S.;Hu, C.; Wang, Z. L. Triboelectric Nanogenerator for Harvesting Vibration Energy in Full Space and as Self - Powered Acceleration Sensor. *Adv. Funct. Mater.* 2014, 24, 1401-1407.
- [17] Decarpigny, J.-N.;Hamonic, B.; Wilson Jr, O. B. The design of low frequency underwater acoustic projectors: present status and future trends. *IEEE J. Oceanic Eng.* 1991, 16, 107-122.
- [18] Fukada, E. History and recent progress in piezoelectric polymers. *IEEE T. Ultrason. Ferr.* 2000, 47, 1277-1290.
- [19] Bucaro, J.;Dardy, H.; Carome, E. Fiber optic hydrophone. *J. Acoust. Soc. Am.* 1977, 62, 1302-1304.
- [20] Niu, S.;Wang, S.;Lin, L.;Liu, Y.;Zhou, Y. S.;Hu, Y.; Wang, Z. L. Theoretical study of contact-mode triboelectric nanogenerators as an effective power source. *Energ. Environ. Sci.* 2013, 6, 3576-3583.
- [21] Kundu, T. Acoustic source localization. *Ultrasonics* 2014, 54, 25-38.

Figures and figure captions

Figure 1. Device structure of an organic film TENG. (a) The schematic diagram. (b) Photograph of a fabricated TENG. (c) SEM image of PTFE surface with etched nanowires structure.

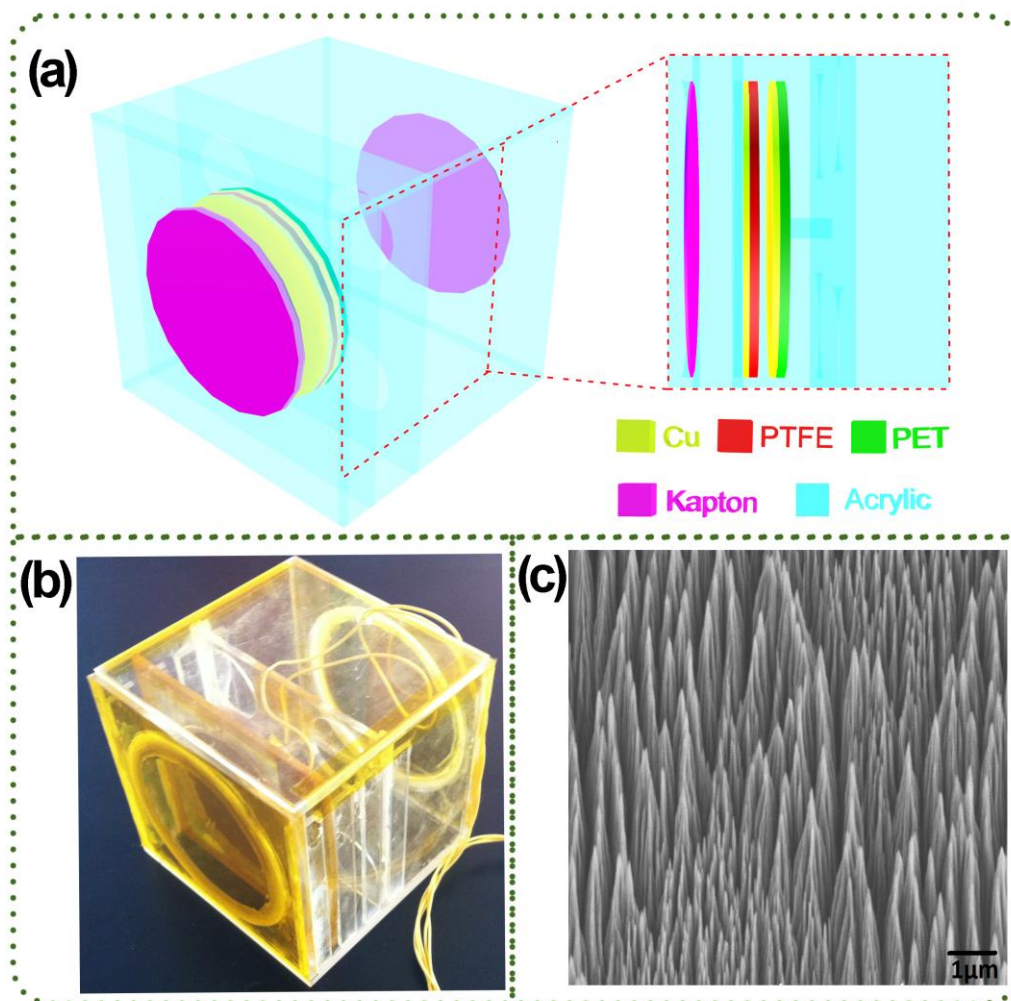


Figure 2. Working mechanism of the TENG. (a) Schematic diagram showing a TENG in working status. The PTFE thin film will oscillate with alternately compressed and expanded air while the PET film stays still. (b-e) Full cycle of the electricity generation process.

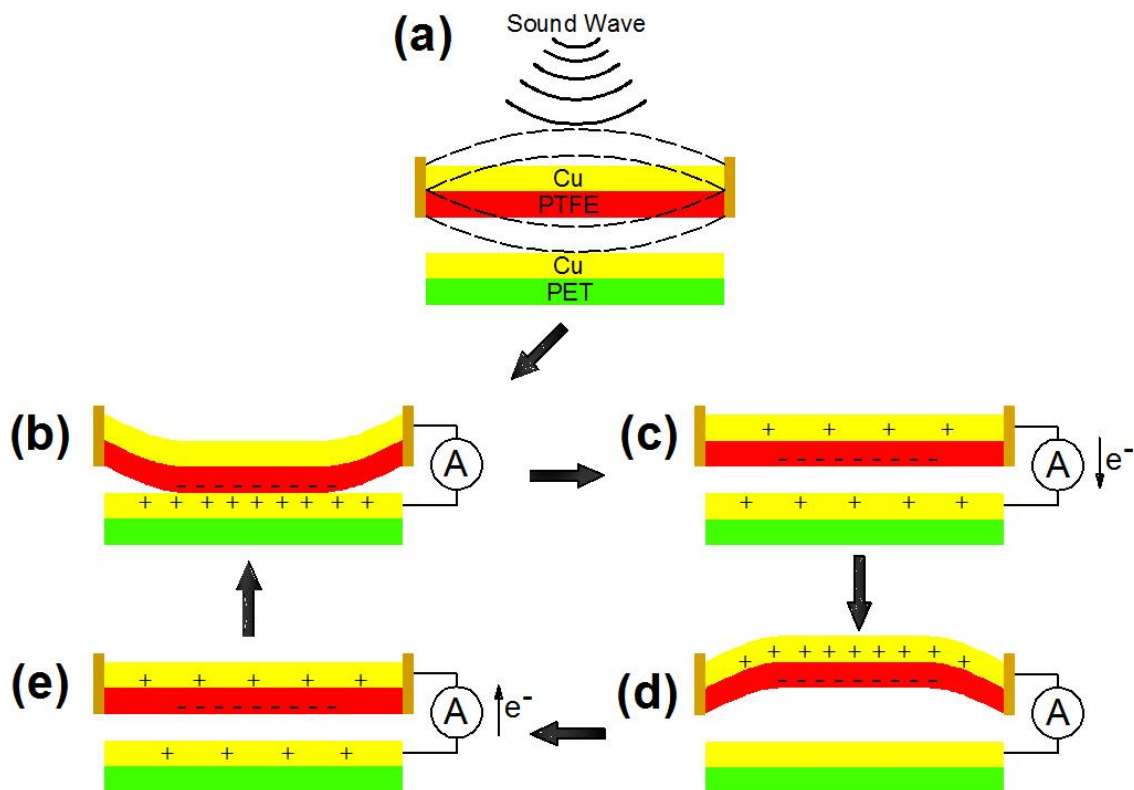


Figure 3. Electrical measurement of TENG underwater. (a) and (b) The frequency response of the TENG's output performance. (c) Open-circuit voltage and (d) Short-circuit current at its resonant frequency of 110Hz under acoustic pressure of 144dB_{SPL}. Open-circuit voltage as a function of (e) acoustic pressures and (f) distance.

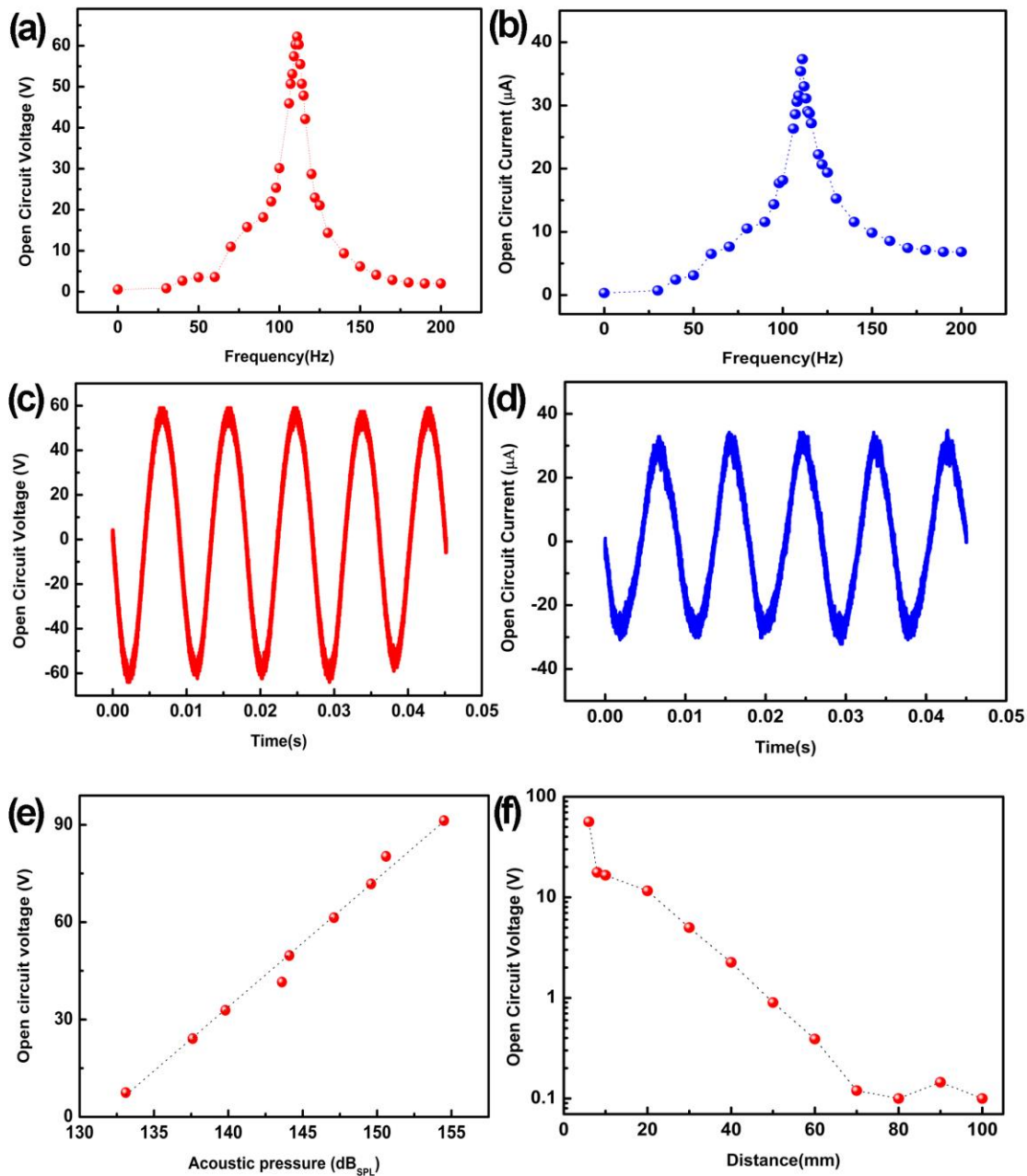


Figure 4. Acoustical performance evaluation of the TENG at a depth of 0.4m underwater. (a) Directional pattern. (b) Sensitivity.

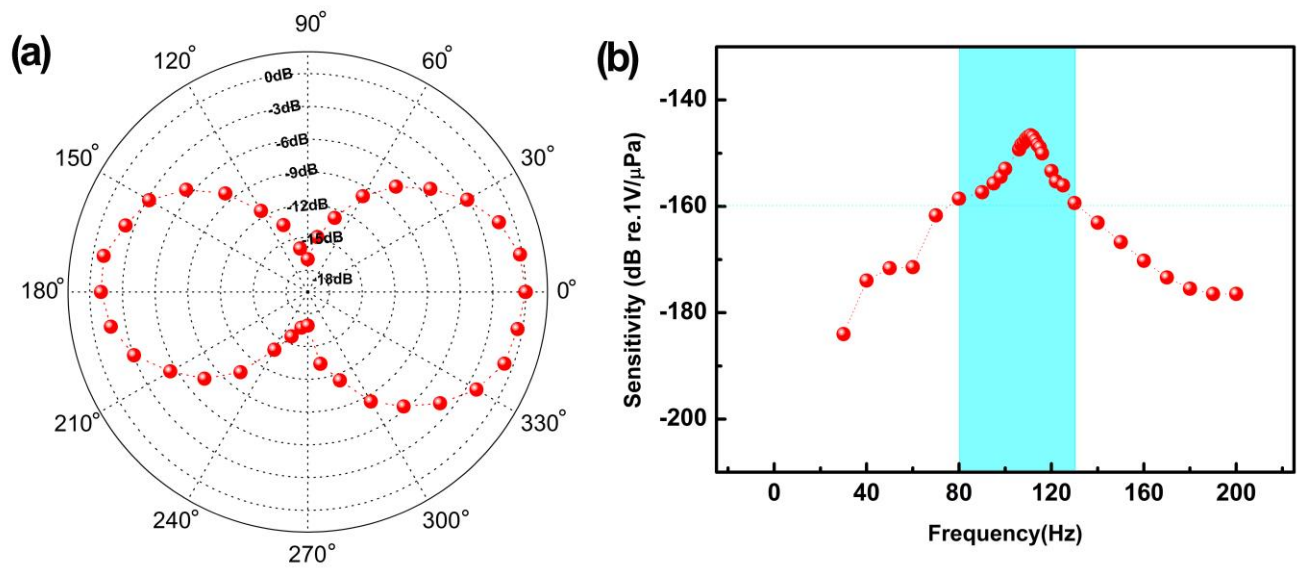
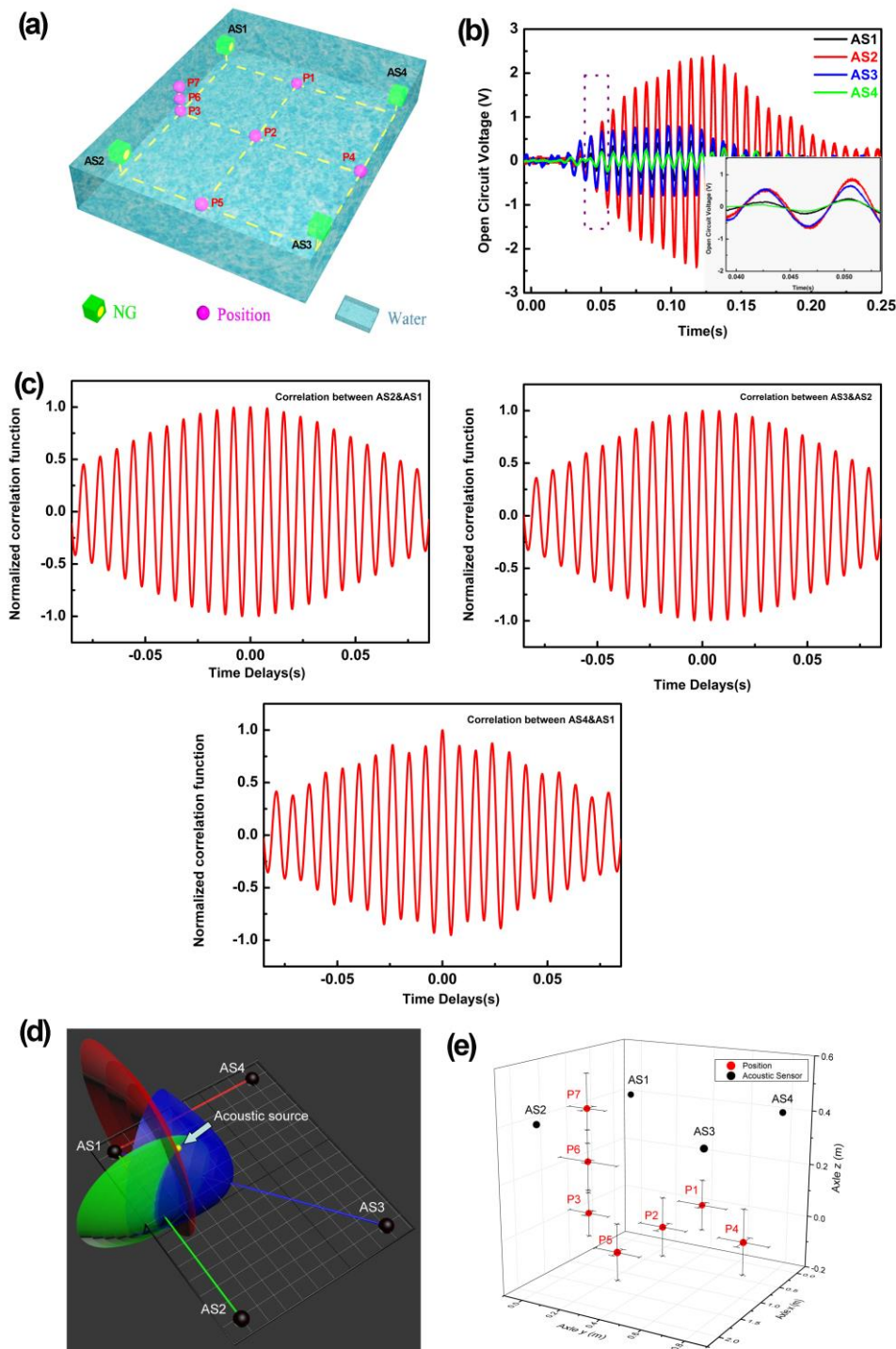


Figure 5. Demonstration of the organic film TENG acting as an active sensor for acoustic source localization underwater. (a) Schematic illustrations and (b) Acquired acoustic signals from the four TENGs when acoustic source works. (c) Correlation functions of the acquired acoustic signals from AS₁, AS₂, AS₃ and AS₄. (d) Photograph showing the working mechanism of TENG for acoustic source localization. (e) Comparison of the measured location and actual location of the vibration source and corresponding location error.



Electronic Supplementary Material

Self-Powered Acoustic Source Locator in Underwater Environment Based on Organic Film Triboelectric Nanogenerator

Aifang Yu^{1†}, Ming Song^{1†}, Yan Zhang¹, Yang Zhang¹, Libo Chen¹, Junyi Zhai¹ (✉) and Zhong Lin Wang^{1,2} (✉)

¹Beijing Institute of Nanoenergy and Nanosystems, Chinese Academy of Sciences, Beijing, 100083, China.

²School of Material Science and Engineering, Georgia Institute of Technology, Atlanta, Georgia 30332, USA.

[†] Authors with equal contribution and authorship order determined by coin toss.

Supporting materials

Table S1. Tab. S1 in the ESM is the position coordinates of acoustic sources (Ps) and active sensors (ASs).

Figure S1. Fig. S1 in the ESM is acquired acoustic signals from the four ASs when acoustic source is settled with various distances to the ASs

Position	Coordinate(cm)
AS1	(0, 0, 0)
AS2	(190, 0, 0)
AS3	(190,76,0)
AS4	(0, 76,0)
P1	(47,38,-18)
P2	(100,38,-18)
P3	(100, 0, -18)
P4	(100,76,-18)
P5	(153,38,-18)
P6	(100, 0, -12)
P7	(100, 0, -7)

